

The Impact of Gate Recess on the H₂ Detection Properties of Pt-AlGaN/GaN HEMT Sensors

Sokolovskij, Robert; Zhang, Jian; Zheng, Hongze; Li, Wenmao; Jiang, Yang; Yang, Gaiying; Yu, Hongyu; Sarro, Pasqualina M.; Zhang, Guoqi

Publication date

2020

Document Version

Final published version

Published in

IEEE Sensors

Citation (APA)

Sokolovskij, R., Zhang, J., Zheng, H., Li, W., Jiang, Y., Yang, G., Yu, H., Sarro, P. M., & Zhang, G. (2020). The Impact of Gate Recess on the H₂ Detection Properties of Pt-AlGaN/GaN HEMT Sensors. *IEEE Sensors*, 20(16), 8947-8955. <http://10.1109/JSEN.2020.2987061>

Important note

To cite this publication, please use the final published version (if applicable). Please check the document version above.

Copyright

Other than for strictly personal use, it is not permitted to download, forward or distribute the text or part of it, without the consent of the author(s) and/or copyright holder(s), unless the work is under an open content license such as Creative Commons.

Takedown policy

Please contact us and provide details if you believe this document breaches copyrights. We will remove access to the work immediately and investigate your claim.

Green Open Access added to TU Delft Institutional Repository

'You share, we take care!' - Taverne project

<https://www.openaccess.nl/en/you-share-we-take-care>

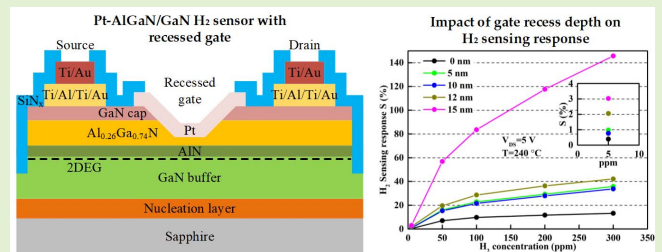
Otherwise as indicated in the copyright section: the publisher is the copyright holder of this work and the author uses the Dutch legislation to make this work public.

The Impact of Gate Recess on the H₂ Detection Properties of Pt-AlGaN/GaN HEMT Sensors

Robert Sokolovskij^{ID}, Jian Zhang, Hongze Zheng, Wenmao Li, Yang Jiang, Gaiying Yang, Hongyu Yu^{ID},
Senior Member, IEEE, Pasqualina M. Sarro, Fellow, IEEE, and Guoqi Zhang, Fellow, IEEE

Abstract—The present work reports on the hydrogen gas detection properties of Pt-AlGaN/GaN high electron mobility transistor (HEMT) sensors with recessed gate structure. Devices with gate recess depths from 5 to 15 nm were fabricated using a precision cyclic etching method, examined with AFM, STEM and EDS, and tested towards H₂ response at high temperature. With increasing recess depth, the threshold voltage (V_{TH}) shifted from -1.57 to 1.49 V. A shallow recess (5 nm) resulted in a 1.03 mA increase in signal variation (ΔI_{DS}), while a deep recess (15 nm) resulted in the highest sensing response (S) of 145.8% towards 300 ppm H₂ as compared to reference sensors without gate recess. Transient measurements demonstrated reversible H₂ response for all tested devices. The response and recovery time towards 250 ppm gradually decreased from 7.3 to 2.5 min and from 29.2 to 8.85 min going from 0 nm to 15 nm recess depth. The power consumption of the sensors reduced with increasing recess depth from 146.6 to 2.95 mW.

Index Terms—AlGaN/GaN, HEMT, H₂ sensor, platinum, gate recess, cyclic etching, enhancement mode.



Manuscript received November 29, 2019; revised March 12, 2020; accepted April 6, 2020. Date of publication April 10, 2020; date of current version July 17, 2020. This work was supported in part by the Shenzhen Municipal Council of Science and Innovation and Shenzhen Institute of the Third Generation Semiconductors, Basic Research Institution of City of Shenzhen under Grant JCYJ20170412153356899 and Grant JCYJ20180305180619573 and in part by the Guangdong Science and Technology Department under Grant 2019B010128001 and Grant 2019B010142001. The associate editor coordinating the review of this article and approving it for publication was Dr. Chang-Soo Kim. (Corresponding authors: Hongyu Yu; Guoqi Zhang.)

Robert Sokolovskij is with the School of Microelectronics, Southern University of Science and Technology (SUSTech), Shenzhen 518055, China, and also with the Department of Microelectronics, Delft University of Technology, 2628 CD Delft, The Netherlands (e-mail: r.sokolovskij@tudelft.nl).

Jian Zhang is with the State Key Laboratory of ASIC and System, School of Microelectronics, Fudan University, Shanghai 200433, China (e-mail: zhsxh@qq.com).

Hongze Zheng, Wenmao Li, Yang Jiang, and Hongyu Yu are with the School of Microelectronics, Southern University of Science and Technology (SUSTech), Shenzhen 518055, China, also with the Key Laboratory of the Third Generation Semi-Conductor, Southern University of Science and Technology (SUSTech), Shenzhen 518055, China, also with the GaN Device Engineering Technology Research Center of Guangdong, Shenzhen 518055, China, also with the Shenzhen Institute of Wide-bandgap Semiconductors, Shenzhen 518100, China, and also with the Engineering Research Center of Integrated Circuits for Next-Generation Communications, Ministry of Education, Shenzhen 518055, China (e-mail: yuhy@sustech.edu.cn).

Gaiying Yang is with the School of Innovation and Entrepreneurship, Southern University of Science and Technology (SUSTech), Shenzhen 518055, China (e-mail: yanggy@sustech.edu.cn).

Pasqualina M. Sarro and Guoqi Zhang are with Department of Microelectronics, Delft University of Technology, 2628 CD Delft, The Netherlands (e-mail: p.m.sarro@tudelft.nl; g.q.zhang@tudelft.nl).

This article has supplementary downloadable material available at <http://ieeexplore.ieee.org>, provided by the authors.

Digital Object Identifier 10.1109/JSEN.2020.2987061

I. INTRODUCTION

THE natural reserves of fossil fuels are depleting and combustion of these hydrocarbons is a major source of greenhouse gases and air pollutants such as CO, CO₂, NO_x, SO_x and particulates that have adverse health effects [1]. Hydrogen is a clean, renewable synthetic fuel that is widely adopted in spacecraft propulsion systems by several nations [2]. A number of technological hurdles still have to be resolved to advance H₂ utilization for personal and commercial vehicles. Storage and transportation of gaseous or liquid H₂ is challenging due to its physical and chemical properties. It is an odorless and colorless gas with high diffusivity, low boiling point of -253 °C and broad flammability range 4–75% in air [3]. Therefore, sensors capable of detecting a wide range of hydrogen concentrations are of critical importance for monitoring and prevention of leakage.

Various types of H₂ sensors including optical, electrochemical, acoustic, catalytic and chemi-resistive have been developed over the last few decades [4]–[6]. The later type of transducer has been comprehensively investigated. Metals, polymers, carbon-based materials and metal oxide semiconductors (MOS) have been employed as H₂ sensitive layers. Utilizing MOS-based nanostructures (nanowires, nanosheets, nanospheres etc.) and carbon materials (carbon nanotubes, graphene) resulted in a further enhancement in gas response due to increased surface-to-volume ratio, compared to their thin film equivalents [7].

Field effect devices such as MOS capacitors, Schottky diodes and MOSFETs are extensively studied for H₂ sensing ever since the first Si-FET with Pd gate was demonstrated [8].

The narrow energy bandgap of Si limits the maximum operating temperature of MOSFETs to approximately 200 °C. Moreover, FET-type sensors often suffer from baseline drift due to contaminants present in the gate oxide and hydrogen induced drift which results in very long recovery time [9].

Other semiconductor materials including GaAs [10], AlGaAs [11], InAlAs [12] or SiC [13] were investigated for H₂ sensor applications in order to improve sensing characteristics and operate in harsh environments. Wide bandgap gallium nitride (GaN) has attracted immense interest for developing electronic devices [14] and next generation high electron mobility transistor (HEMT)-based sensors [15] due to its superior electronic, chemical, thermal and mechanical properties. Furthermore, AlGaN/GaN heterojunctions exhibit strong polarization effects, forming a high carrier density and mobility two-dimensional electron gas (2DEG) channel at the interface. Since the initial report of the AlGaN/GaN HEMT H₂ sensor with Pt gate [16] several modifications to the sensor structure have been studied in order to enhance the sensing characteristics [17]–[20]. Detection of numerous other gases has also been reported with GaN-based sensors [21]–[24].

A specific and widely studied modification of AlGaN/GaN HEMTs is the recess etching of the thin (20–30 nm) AlGaN barrier in order to achieve enhancement-mode (E-mode) operation [25] and to reduce the contact resistance of Au-free, CMOS compatible ohmic contacts [26]. Nevertheless, only few reports have investigated the impact of AlGaN barrier recess on sensing performance of HEMT-based sensors. An open gate, two-terminal AlGaN/GaN NO₂ sensor with varying barrier recess depths was reported by [27]. Thinning the AlGaN barrier was found to increase the response to low NO₂ concentrations. A pH and glucose biosensor with recessed barrier and functionalized with ZnO nanorods was demonstrated by [28]. Photoelectrochemical (PEC) etching using H₃PO₄ solution and He-Cd laser was utilized to partially recess the AlGaN barrier as well as to form a gate oxide layer consisting of Al₂O₃/Ga₂O₃. Sensitivity towards pH and glucose was increased using the recessed structure. To our knowledge, three-terminal HEMT-based gas sensors with recessed barrier and catalytic metal gate have not been studied so far. Several methods of AlGaN/GaN recess etching have been previously demonstrated including low power inductively coupled plasma reactive ion etching (ICP-RIE) using Cl₂/BCl₃ plasma, digital etching, PEC and thermal oxidation [29]–[32].

In this work, we expand upon our initial results [33] on the impact of gate recess on H₂ sensing characteristics of Pt-AlGaN/GaN HEMT-based sensors. A modified cyclic recess etching process [34] was utilized to fabricate sensors with several depths of gate recess. To analyze static and transient characteristics of these sensors, measurements in H₂ gas ambient with controlled concentrations in the ppm range were conducted.

II. EXPERIMENTAL

A. Sensor Micro-Fabrication

The starting AlGaN/GaN heterostructure, grown by MOCVD on 2-inch c-plane sapphire wafers, was supplied by

a commercial vendor. Starting from the substrate the epitaxy consists of a proprietary nucleation layer, a 1.8 μm GaN buffer layer, a 1 nm AlN spacer, a 21 nm Al_{0.26}Ga_{0.74}N barrier and a 1.5 nm GaN capping layer. The process started with wafer cleaning using piranha solution (3:1/H₂SO₄:H₂O₂) followed by acetone, isopropanol and DI water rinsing to remove any particulates or organic contaminants. Mesa etching was then performed using ICP-RIE with BCl₃/Cl₂ plasma to the depth of 100 nm. Afterwards 200 nm of PECVD SiO₂ were deposited and patterned by buffered oxide etching (BOE) to be used as hard mask for barrier recess. Plasma oxidation of the GaN cap and AlGaN barrier layers was performed in a Naura GSE 200 Plus ICP-RIE tool. The recipe parameters were similar to those used in [34], with ICP power 450 W, O₂ flow rate of 40 sccm, base pressure 8 mtorr and 180 s oxidation time. The RF power was varied in the range of 20–75 W to modify the oxidation depth rate per cycle. A solution of 1:4/HCl:H₂O was used to etch the formed plasma oxide. Sensors with four different recess depths were fabricated for comparison, denoted as samples B, C, D and E, while sample A was the reference sample without gate recess. The SiO₂ mask was then removed by BOE etching. The ohmic contact patterns were formed by photolithographic patterning, e-beam evaporation of Ti/Al/Ti/Au (20/110/40/50 nm) and lift-off. Prior to the metal deposition a dip in 1:4/HCl:H₂O was done in order to remove any native oxide. Rapid thermal annealing (RTA) at 850 °C for 45 s in N₂ ambient was performed to lower the contact resistance. A 10 nm-thick layer of Pt was then e-beam deposited and patterned to form the sensing gate electrode. Afterwards the interconnect bi-layer of Ti/Au with thickness 20/300 nm was processed by e-beam evaporation and lift-off. Device passivation was then carried out by depositing 200 nm of PECVD SiN_x in order to protect the GaN surface and metal interconnects from scratches and contamination. The SiN_x was then patterned by a combination of ICP-RIE followed by wet BOE etching to expose the Pt gate to the ambient and the contact pads for wire bonding. The schematic cross-section view of the HEMT-sensor structure with a recessed gate electrode is shown in Fig. 1a and an optical micrograph of the processed sensor (top view) in Fig. 1b. The dimensions of the gate electrode exposed to the ambient were 4 μm × 400 μm, the source-gate and gate-drain spacing was 6 μm.

B. Sensor Testing

The fabricated sensors were wire-bonded to ceramic substrates and placed in a stainless steel 100 ml volume chamber equipped with a heater and a humidity sensor. The concentration of the test gas and the relative humidity (RH) inside the testing chamber were controlled with mass flow controllers using a commercial gas mixing system from Beijing Elite Tech Co. The test gas was supplied from H₂ cylinders with known concentration, diluted in N₂. The background gas was synthetic air (O₂/N₂ = 21%/79%) and RH~0%. The combined total gas flow was set to 400 sccm. Electrical connections to the sensors were made with probe needles inside the test chamber and current-voltage (*I-V*) characteristics were measured using two Keithley 2450 sourcemeters. A schematic

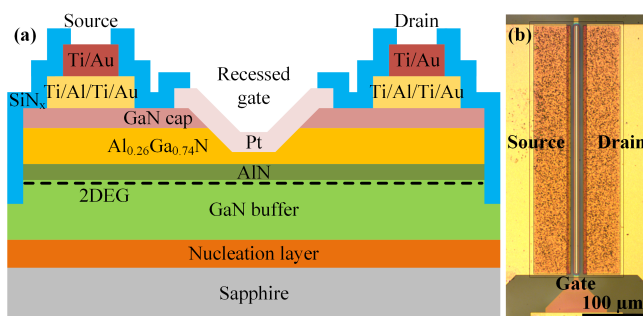


Fig. 1. Schematic cross-section of the recessed gate Pt-AlGaIn/GaN HEMT H₂ sensor (a). Optical micrograph (top view) of the fabricated sensor (b).

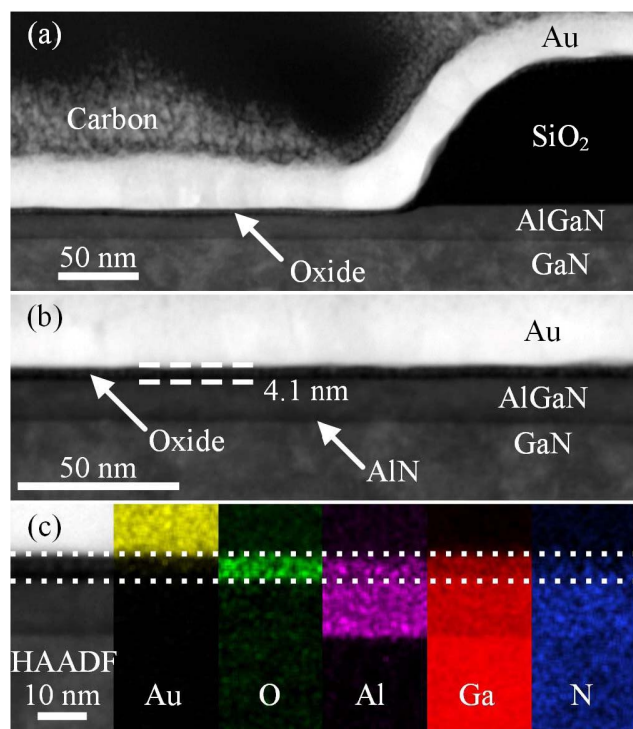


Fig. 2. Cross-section STEM images of (a) the pattern edge exposed to oxygen plasma treatment and (b) a magnified view of the oxidized AlGaIn surface. (c) EDS element mapping of the oxygen plasma exposed region. The area between the dashed lines indicates the oxidized AlGaIn surface.

diagram of the gas testing system is shown in fig. S1 and an image of a sensor mounted in the testing chamber in fig. S2. Prior to H₂ sensing, as fabricated sensors underwent a burn-in process at 260 °C for 12 h in order to reduce the baseline signal drift.

III. RESULTS AND DISCUSSION

A. Gate Recess Characterization

In order to validate the cyclic nature of the two-step barrier recess process, scanning transmission electron microscopy (STEM) imaging was conducted on test samples using FEI Talos STEM with 200 kV acceleration voltage. Fig. 2a shows the cross-sectional view of the patterned sample after 180 s ICP-RIE oxidation at 40 W RF power. The Au and carbon layers were deposited to protect the chip surface during TEM sample preparation using focused ion beam (FIB). A thin

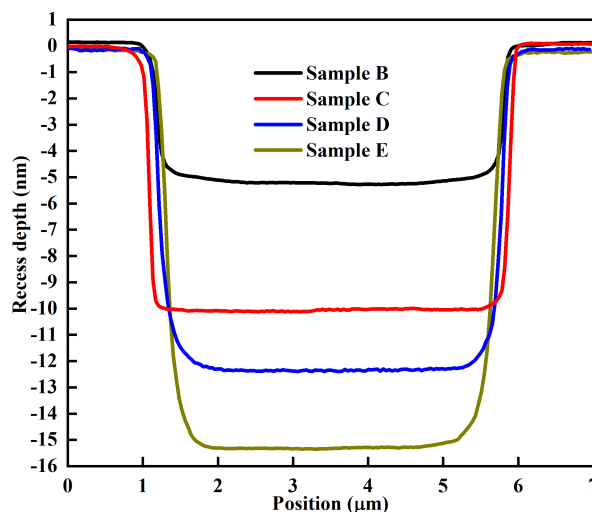


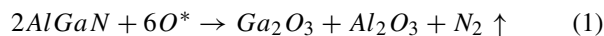
Fig. 3. Depth profiles obtained by AFM scans of samples B, C, D and E across 5 μm wide test trenches.

TABLE I

RF POWER OF OXIDATION RECIPES, ETCH DEPTH AND RECESSED REGION RMS SURFACE ROUGHNESS OF SENSORS B-E, MEASURED BY AFM

Sensor	RF power (W)	Recess depth (nm)	RMS (nm)
B	20+20	5.4	0.57
C	75+40	10.1	0.51
D	75+75	12.3	0.54
E	75+75+35	15	0.56

layer of oxide has formed on the plasma exposed surface and some of the AlGaIn layer was consumed in the process. The thickness of the oxide was 4.1 nm as determined from the magnified view of the oxidized area shown in fig. 2b. The results of energy dispersive spectroscopy (EDS) analysis are shown in fig. 2c. The presence of O, Al and Ga is clearly observed in the oxidized film, whereas N concentration is diminished, which suggests that a Ga₂O₃/Al₂O₃ layer was formed. The likely reaction mechanism of the ICP plasma oxidation is:



where O* are the excited oxygen plasma atoms. The depth of the recess was measured by atomic force microscopy (AFM) using Bruker Dimension Edge. The depth profiles of the barrier recess across a 5 μm wide test structure are shown in fig. 3. The RF power settings of the plasma oxidation recipes, the measured recess depth and trench RMS surface roughness of samples B–E are summarized in Table I. A low RMS roughness was measured for all depths which indicates a minimal AlGaIn surface damage during barrier etching. Samples B–D required two oxidation/etching cycles to obtain the desired etching depth, while three cycles were used for sample E. The cross-section STEM image of the non-recessed and recessed AlGaIn regions of sample E is shown in fig. 4a. Cyclic etching resulted in a tapered recess profile and smooth surface. The remaining AlGaIn thickness was approximately 2.3 nm. An interfacial layer of about 2 nm was observed between the Pt gate and the AlGaIn layer. EDS analysis,

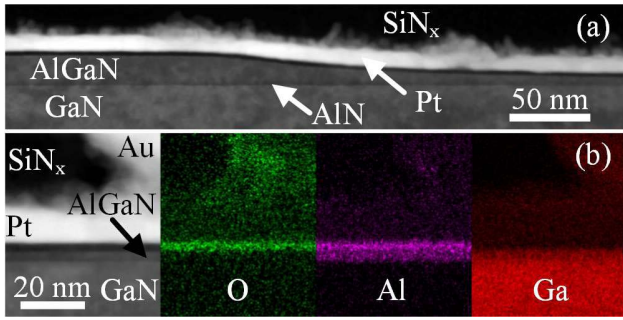


Fig. 4. (a) Cross-section STEM image of the non-recessed and recessed regions of the AlGaIn barrier. (b) EDS element mapping of the recessed region under the Pt gate electrode.

shown in fig. 4b, indicates that this layer was O and Al rich, likely Al_2O_3 . It is possible that this oxide was formed due to exposure to atmosphere and during contact RTA, as residual H_2O and O_2 may be present in the N_2 atmosphere of the annealing chamber [35]. No oxide etching treatments were performed prior to Pt gate metal deposition, as the interfacial oxide enhances H_2 detection [24], [36].

B. Gas Sensing Measurements

Electrical measurements were conducted in order to determine the influence of the gate recess depth on the characteristics of the studied sensors prior to gas sensing experiments. The transfer curves ($I_{DS}-V_{GS}$) of sensors A-E at 30°C and $V_{DS} = 7\text{ V}$ are shown in fig. 5a. A clear shift of the curves towards positive values is observed with increasing depth of barrier recess. The threshold voltages (V_{TH}) of these devices were extracted by fitting a tangent line at the point of maximum transconductance ($g_{m,max}$) to the x-axis intercept (i.e. $I_{DS} = 0$) [37]. The $g_{m,max}$ values for sensors A-E are given in Table II. Fig. 5b shows the shift of V_{TH} with increasing recess depth. V_{TH} increased from -1.57 V for the non-recessed sensor A to $V_{TH} = 1.49\text{ V}$ for sensor E with 15 nm recess depth, which resulted in enhancement mode device. The V_{TH} of an AlGaIn/GaN HEMT can be expressed as:

$$V_{TH} = \phi_B - \Delta E_C - \frac{qN_D d_{AlGaIn}^2}{2\epsilon_{AlGaIn}} - \frac{qn_s}{\epsilon_{AlGaIn}} d_{AlGaIn} \quad (2)$$

where ϕ_B is the gate Schottky barrier height, ΔE_C is the conduction band discontinuity between AlGaIn and GaN, q is the elementary charge, n_s is the sheet carrier density of the 2DEG and N_D , d_{AlGaIn} and ϵ_{AlGaIn} are the doping concentration, thickness and dielectric permittivity of AlGaIn, respectively. The barrier recess etching reduces the n_s and increases the gate capacitance ($C_g = \epsilon_{AlGaIn}/d_{AlGaIn}$), leading to the observed positive V_{TH} shift.

Sensing characteristics of the fabricated sensors were examined by exposing them to increasing concentrations of H_2 in dry air (RH \sim 0%) at 240°C . The measured transfer characteristics of sensors A-E at $V_{DS} = 7\text{ V}$ exposed to 5-300 ppm H_2 are shown fig. 6a-e. All devices demonstrated a response to low H_2 concentrations as evident from the V_{TH} shift towards more negative values. The threshold voltage shift ($\Delta V_{TH} = V_{TH,air} - V_{TH,H_2}$) of the tested sensors with

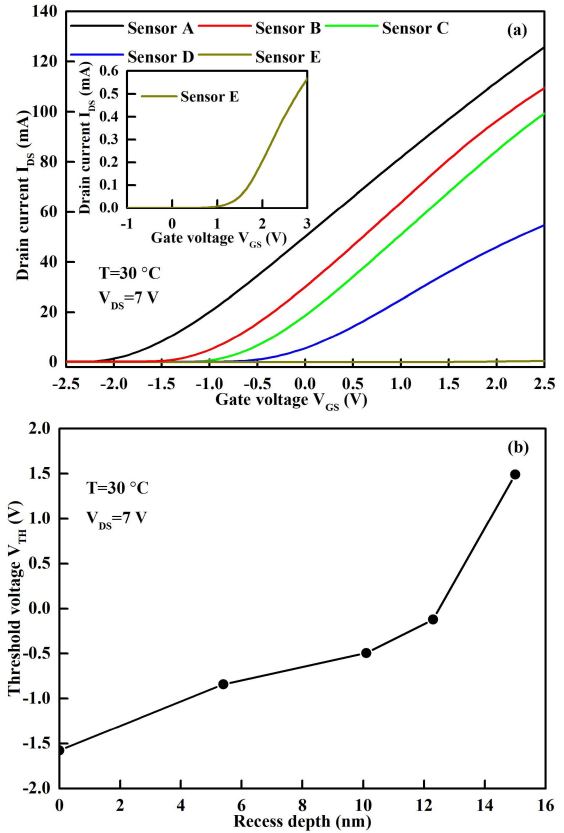


Fig. 5. (a) Transfer characteristics ($I_{DS}-V_{GS}$) of sensors A-E at 30°C . The inset shows the magnified view for sensor E. (b) Measured threshold voltage values with increasing depth of barrier recess.

TABLE II

MAXIMUM TRANSCONDUCTANCE VALUES OF SENSORS A-E AT 30 AND 240°C

Sensor	$g_{m,max}$ (mS) at 30°C	$g_{m,max}$ (mS) at 240°C
A	31.8	12.26
B	34.6	14.66
C	34.1	14.05
D	22.4	9.02
E	0.4	0.32

increasing recess depth upon exposure to 300 ppm of H_2 is shown in fig. 6f. Compared to the reference sensor A the ΔV_{TH} was higher for sensors B and C, while it reduced for sensors D and E, which corresponds to the measured maximum transconductance ($g_{m,max}$) values at 240°C (Table II). The corresponding output characteristics upon H_2 exposure are shown in fig. 7. The gate voltage was stepped from -3 V to 1 V with 1 V increments for sensors A-D and from -1 V to 3 V for sensor E. The devices still maintained proper HEMT characteristics at high temperature above the Si-based FET limit. The saturation drain current decreased with deeper recess depth due to lowering of the electron density under the gate electrode and increase in the channel resistance (R_{ch}) according to [25]:

$$R_{ch} = \frac{L_g t_r}{\mu \epsilon_{AlGaIn} (V_{GS} - V_{TH} - \phi_B)} \quad (3)$$

where L_g is the gate length, t_r the thickness of the AlGaIn barrier under the gate and μ is the electron mobility. The relation

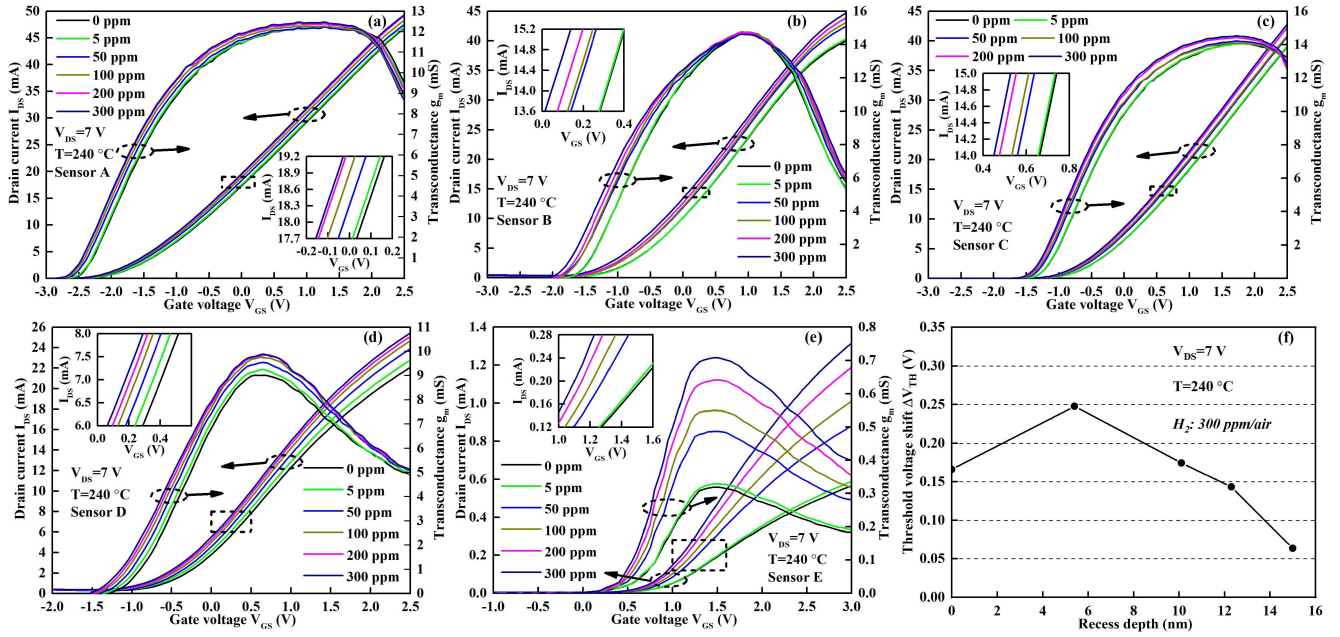


Fig. 6. Transfer characteristics (I_{DS} - V_{GS}) of (a) sensor A, (b) sensor B, (c) sensor C, (d) sensor D and (e) sensor E exposed to different H₂ concentrations at 240 °C. The insets show the magnified view of the dashed box area. (f) The threshold voltage shift (ΔV_{TH}) from air to 300 ppm H₂ as a function of recess depth.

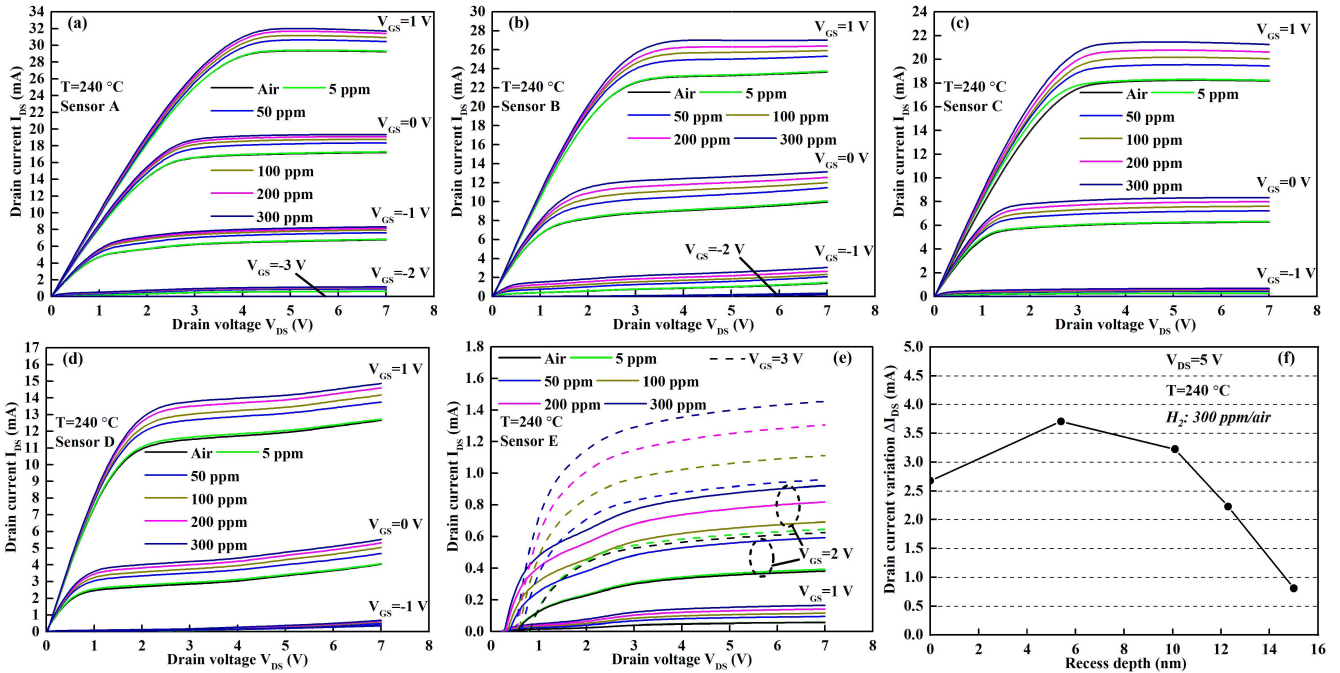


Fig. 7. Output characteristics (I_{DS} - V_{DS}) of (a) sensor A, (b) sensor B, (c) sensor C, (d) sensor D and (e) sensor E exposed to different H₂ concentrations at 240 °C. (f) The drain current variation (ΔI_{DS}) from air to 300 ppm H₂ as a function of recess depth.

between the 2DEG density of the non-recessed (n_s) and recessed (n_{sr}) region can be expressed as:

$$n_{sr} = n_s \left(1 - \frac{t_{cr}}{t_r}\right) \quad (4)$$

where t_{cr} is the critical thickness of AlGaIn to form the 2DEG [38] and is expressed as:

$$t_{cr} = \frac{(\phi_B - \Delta E_C)\epsilon_{AlGaIn}}{qn_s} \quad (5)$$

The dependence of threshold voltage on the barrier thickness can then be expressed as:

$$V_{TH} = \phi_B + \frac{qn_s}{\epsilon_{AlGaIn}}(t_{cr} - t_r) \quad (6)$$

Compared with other sensors the drain current of device E reduced substantially. This is attributed to significant reduction of 2DEG density as the barrier was recessed down to near critical thickness (t_{cr}). Furthermore, the voltage difference

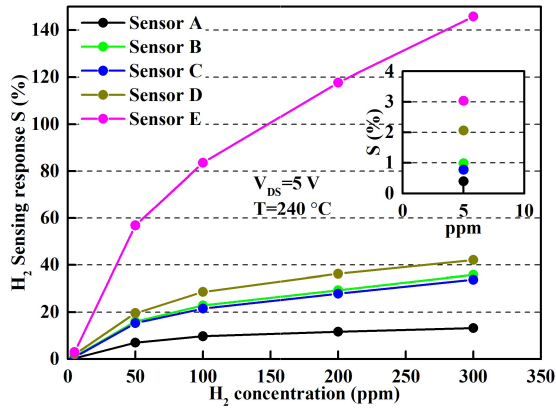


Fig. 8. H₂ sensing response of sensors A-E at 240 °C. The $V_{GS} = 0$ V for A-D, and $V_{GS} = 2$ V for sensor E. The inset shows the magnified S toward 5 ppm.

($V_{GS} - V_{TH}$) is reduced for E-mode HEMT leading to additional increase of the channel resistance (R_{ch}). Biasing the device at higher gate voltage leads to forward bias gate leakage as evident from the shift of the drain voltage axis crossing point and hence reverse current flow at low V_{DS} (see fig. 7e). The drain current (I_{DS}) increased upon H₂ exposure down to 5 ppm in air. The detection mechanism is based on catalytic dissociation of H₂ molecules into 2H atoms at the surface of the Pt gate. Some of these atoms rapidly diffuse through the Pt towards the metal-semiconductor interface and form a dipolar layer. The dipoles cause a reversible lowering of the Pt work function, which results in the observed negative threshold voltage shift (ΔV_{TH}) and output current increase (ΔI_{DS}) [39].

To characterize and compare the H₂ sensing performance of the studied sensors the drain current variation (ΔI_{DS}) and sensing response (S) were determined. The S is defined as:

$$S(\%) = \frac{I_{DS,H_2} - I_{DS,air}}{I_{DS,air}} \times 100\% = \frac{\Delta I_{DS}}{I_{DS,air}} \times 100\% \quad (7)$$

where I_{DS,H_2} and $I_{DS,air}$ is the drain current magnitude under H₂ containing and air ambient, respectively. The drain current variation (ΔI_{DS}) as a function of recess depth is shown in fig. 7f. The drain bias of all devices was $V_{DS} = 5$ V and the gate bias (V_{GS}) was 1 V for devices A-D and 3 V for device E. Compared to sensor A the ΔI_{DS} increased from 2.68 mA to 3.71 mA for sensor B and 3.22 mA for sensor C when exposed to 300 ppm H₂ and decreased with deeper recess. The H₂ sensing response (S) of the tested sensors is shown in fig. 8. The $V_{DS} = 5$ V for all sensors and $V_{GS} = 0$ V for sensors A-D and $V_{GS} = 2$ V for sensor E. The S towards 300 ppm of H₂ increased from 13.23 % for sensor A to 35.84, 33.76, 42.15 and 145.77 % for sensors B-E, respectively. An 11x increase in sensing response was obtained for a 15 nm recess depth compared to non-recessed sensor. The increase of sensing response with deeper recess is attributed to the reduction of the baseline signal value in air ($I_{DS,air}$).

Transient response characteristics of the Pt-AlGaN/GaN HEMT sensors at 240 °C towards 10-250 ppm H₂ are shown in fig. 9. The sensors A-D were biased at $V_{GS} = 0$ V and sensor E at $V_{GS} = 1.5$ V, while the $V_{DS} = 5$ V for all tested sensors. The drain current increased immediately after

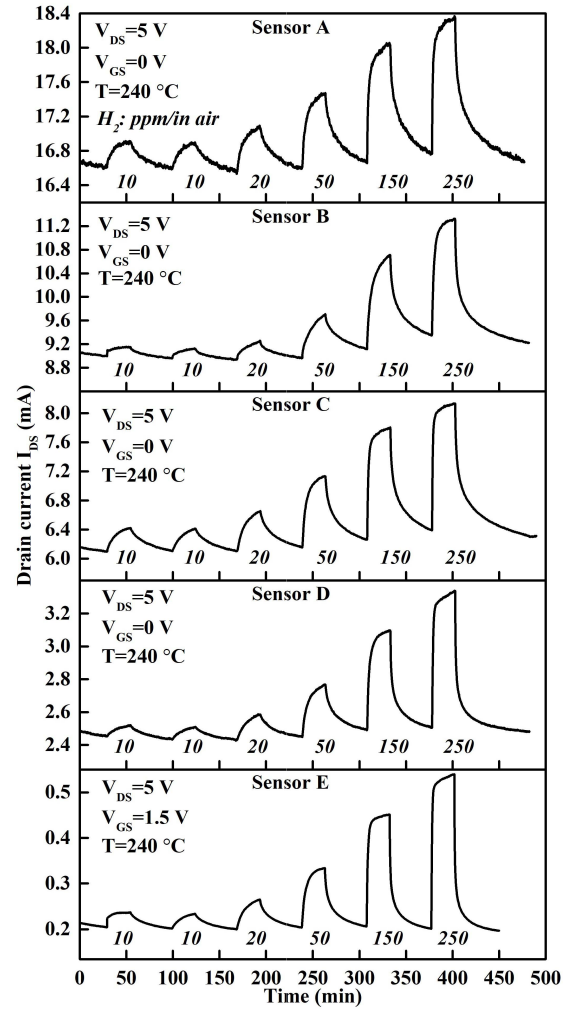


Fig. 9. Transient response characteristics upon injection and purge of H₂ at 240 °C for sensors A-E with increasing depth of recess. The $V_{GS} = 0$ V for sensors A-D and $V_{GS} = 1.5$ V for sensor E.

the gas was introduced into the test chamber. The response (t_{res}) and recovery time (t_{rec}) of the tested sensors towards 250 ppm with increasing recess depth is shown in fig. 10. The t_{res} is defined as the time required for the sensors to reach 90 % of the equilibrium I_{DS} value in H₂ and t_{rec} is the time needed for I_{DS} to return to 10 % above the value in air. Both t_{res} and t_{rec} gradually decreased with thinning the AlGaN barrier. The response time decreased from 7.26 min for non-recessed sensor A to 2.5 min for sensor E with 15 nm recess and the recovery time decreased from 29.2 min to 8.85 min, respectively.

Sensor signal repeatability was studied by exposing them to three successive cycles of 250 ppm H₂ for 25 min followed by air purging for 60 min as shown in fig. 11. Repeatabile sensor signal variation was observed for all sensors, indicating that recessing the barrier does not deteriorate the transient sensor operation and improves the recovery to baseline value in air.

Reducing the power consumption of GaN-HEMT based micro-sensors is crucial for integration into portable and battery powered gas detectors. The comparison of continuous power consumption (P) is presented in fig. 12. The power values were calculated at $V_{DS} = 5$ V and V_{GS} of 0 and

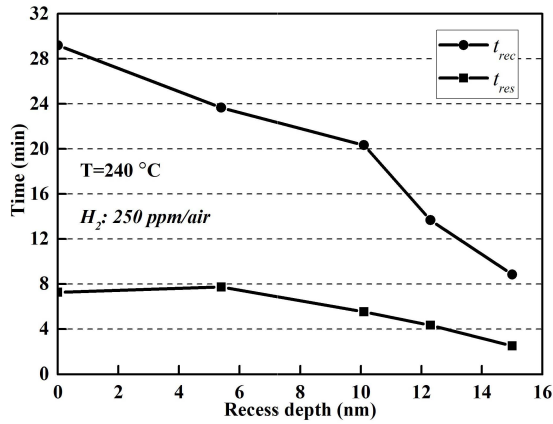


Fig. 10. The response (t_{res}) and recovery (t_{rec}) times of sensors A-E as a function of recess depth. The $V_{GS} = 0$ V for A-D, and $V_{GS} = 1.5$ V for sensor E.

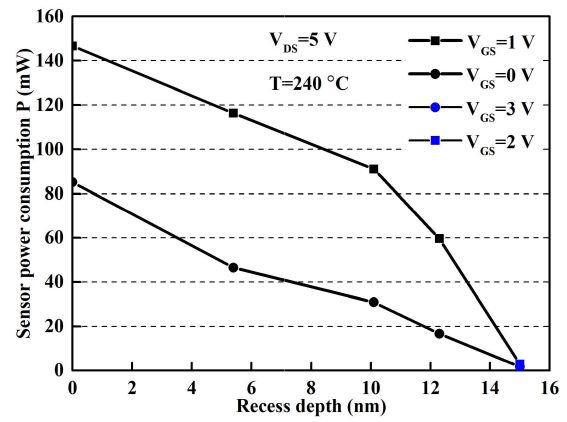


Fig. 12. Power consumption values for sensors A-E at 240 °C and $V_{DS} = 5$ V.

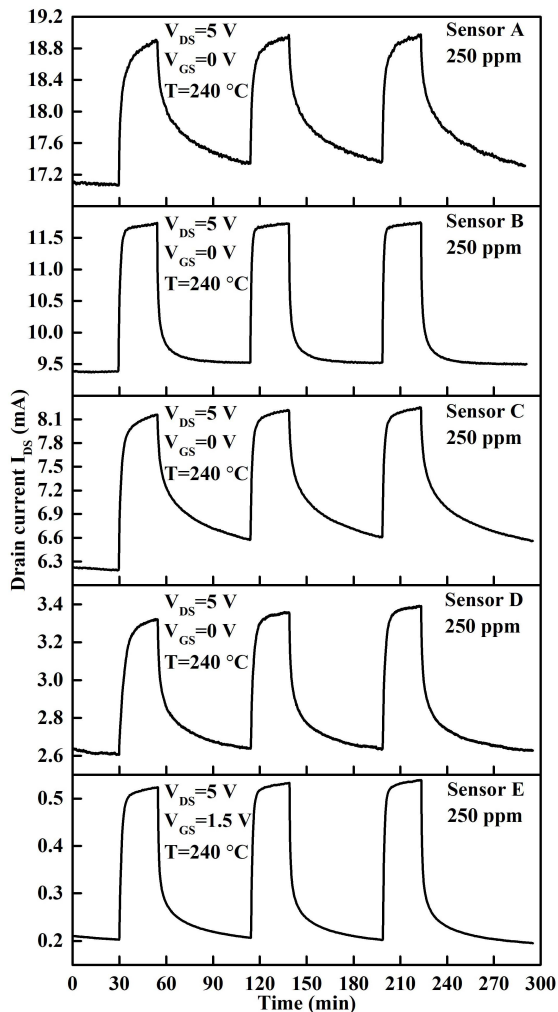


Fig. 11. Repeatability of sensor response upon injection and purge of 250 ppm H₂ at 240 °C for sensors A-E with increasing depth of recess. The $V_{GS} = 0$ V for sensors A-D and $V_{GS} = 1.5$ V for sensor E.

1 V for sensors A-D, while for sensor E the V_{GS} was 2 and 3 V. The power consumption decreased from 85.2 (146.6) mW to 1.8 (2.95) mW when comparing sensors A and E at $V_{GS} 0$ (1) V and 2 (3) V, respectively. The measured decrease

of the power consumption is attributed to the lowering of the baseline drain current value (I_{DS}) due to increased channel resistance for deeper recess depth as indicated from the data reported in fig. 9. The obtained 48x power reduction is significant as additional power would be required to raise the operating temperature of the sensors via integrated microheater in real-world application scenario.

IV. CONCLUSION

The H₂ sensing characteristics of Pt-AlGa_n/Ga_n HEMT sensors with recessed gate structure were analyzed and compared to non-recessed sensors. Sensors with increasing barrier recess depths from 5 to 15 nm were fabricated using the highly controllable, low damage cyclic barrier etching method. The depth and surface roughness of the recessed regions was studied with AFM and the Pt-AlGa_n interface was examined by STEM and EDS. A positive shift of threshold voltage (V_{TH}) from -1.57 V to 1.49 V was obtained going from 0 nm to 15 nm recess depth, due to the lowering of the 2DEG density under the thinner AlGa_n layer under the gate electrode.

High temperature (240 °C) static and transient H₂ sensing characteristics were studied and compared with the baseline sensor. Exposure to H₂ resulted in the increase in drain current (ΔI_{DS}) and negative shift of threshold voltage (ΔV_{TH}). All the tested sensors were able to detect low H₂ concentrations down to 5 ppm in air. The largest ΔI_{DS} and ΔV_{TH} of 3.71 mA and 0.25 V at 300 ppm was obtained for sensors with the 5 nm recess. These values were 1.03 mA and 0.08 V higher than of the reference sensor. The sensing response at 300 ppm gradually increased with recess depth from 13.2 % for non-recessed sensor to 145.8 % for sensor with 15 nm recess depth. Comparing non-recessed and 15 nm recessed sensors the response (recovery) time decreased from 7.3 (29.2) min to 2.5 (8.85) min, respectively. Power consumption of the sensors was effectively reduced by implementing the barrier recess from 146.6 mW to 2.95 mW. Therefore, precisely etching a recess in the barrier layer under the gate electrode is an effective method to enhance the H₂ sensing properties of AlGa_n/Ga_n HEMT based sensors.

ACKNOWLEDGMENT

Parts of the device fabrication and characterization were conducted at Materials Characterization and Preparation Center (MCPC) at SUSTech, and the authors acknowledge the technical support from the engineers at MCPC.

REFERENCES

- [1] M. Kampa and E. Castanas, "Human health effects of air pollution," *Environ. Pollut.*, vol. 151, no. 2, pp. 362–367, Jan. 2008.
- [2] D. Cecere, E. Giacomazzi, and A. Ingenito, "A review on hydrogen industrial aerospace applications," *Int. J. Hydrogen Energy*, vol. 39, no. 20, pp. 10731–10747, Jul. 2014.
- [3] Y. S. H. Najjar, "Hydrogen safety: The road toward green technology," *Int. J. Hydrogen Energy*, vol. 38, no. 25, pp. 10716–10728, Aug. 2013.
- [4] Y.-N. Zhang, H. Peng, X. Qian, Y. Zhang, G. An, and Y. Zhao, "Recent advancements in optical fiber hydrogen sensors," *Sens. Actuators B, Chem.*, vol. 244, pp. 393–416, Jun. 2017.
- [5] T. Häbert, L. Boon-Brett, G. Black, and U. Banach, "Hydrogen sensors—A review," *Sens. Actuators B, Chem.*, vol. 157, no. 2, pp. 329–352, Oct. 2011.
- [6] G. Korotcenkov, S. D. Han, and J. R. Stetter, "Review of electrochemical hydrogen sensors," *Chem. Rev.*, vol. 109, no. 3, pp. 1402–1433, Mar. 2009.
- [7] P. S. Chauhan and S. Bhattacharya, "Hydrogen gas sensing methods, materials, and approach to achieve parts per billion level detection: A review," *Int. J. Hydrogen Energy*, vol. 44, no. 47, pp. 26076–26099, Oct. 2019.
- [8] K. I. Lundström, M. S. Shivaraman, and C. M. Svensson, "A hydrogen sensitive PD gate MOS transistor," *J. Appl. Phys.*, vol. 46, no. 9, pp. 3876–3881, Sep. 1975.
- [9] C. Nylander, M. Armgarth, and C. Svensson, "Hydrogen induced drift in palladium gate metal oxide semiconductor structures," *J. Appl. Phys.*, vol. 56, no. 4, pp. 1177–1188, Aug. 1984.
- [10] L. M. Lechuga, A. Calle, D. Golmayo, P. Tejedor, and F. Briones, "A new hydrogen sensor based on a Pt/GaAs Schottky diode," *Sens. Actuators B, Chem.*, vol. 4, nos. 3–4, pp. 515–518, 1991.
- [11] C. T. Lu, K. W. Lin, H. I. Chen, H. M. Chuang, C. Y. Chen, and W. C. Liu, "A new Pd-oxide- $\text{Al}_{0.3}\text{Ga}_{0.7}\text{As}$ MOS hydrogen sensor," *IEEE Electron Device Lett.*, vol. 24, no. 4, pp. 390–392, Apr. 2003.
- [12] C.-W. Hung *et al.*, "Temperature-dependent hydrogen sensing characteristics of a new Pt/InAlAs Schottky diode-type sensor," *Sens. Actuators B, Chem.*, vol. 128, no. 2, pp. 574–580, Jan. 2008.
- [13] M. T. Soo, K. Y. Cheong, and A. F. M. Noor, "Advances of SiC-based MOS capacitor hydrogen sensors for harsh environment applications," *Sens. Actuators B, Chem.*, vol. 151, no. 1, pp. 39–55, Nov. 2010.
- [14] B. J. Baliga, "Gallium nitride devices for power electronic applications," *Semicond. Sci. Technol.*, vol. 28, no. 7, Jul. 2013, Art. no. 074011.
- [15] S. J. Pearton *et al.*, "Recent advances in wide bandgap semiconductor biological and gas sensors," *Prog. Mater. Sci.*, vol. 55, no. 1, pp. 1–59, Jan. 2010.
- [16] J. Schalwig, G. Müller, M. Eickhoff, O. Ambacher, and M. Stutzmann, "Gas sensitive GaN/AlGaIn-heterostructures," *Sens. Actuators B, Chem.*, vol. 87, no. 3, pp. 425–430, Dec. 2002.
- [17] B. S. Kang *et al.*, "Hydrogen-induced reversible changes in drain current in $\text{Sc}_2\text{O}_3/\text{AlGaIn}/\text{GaN}$ high electron mobility transistors," *Appl. Phys. Lett.*, vol. 84, no. 23, pp. 4635–4637, Jun. 2004.
- [18] C.-C. Huang *et al.*, "On an electroless plating (EP)-based Pd/AlGaIn/GaN heterostructure field-effect transistor (HFET)-type hydrogen gas sensor," *IEEE Electron Device Lett.*, vol. 33, no. 6, pp. 788–790, Jun. 2012.
- [19] S. Jang, P. Son, J. Kim, S.-N. Lee, and K. H. Baik, "Hydrogen sensitive Schottky diode using semipolar (11 $\bar{2}$) AlGaIn/GaN heterostructures," *Sens. Actuators B, Chem.*, vol. 222, pp. 43–47, Jan. 2016.
- [20] S. Jung, K. H. Baik, F. Ren, S. J. Pearton, and S. Jang, "Temperature and humidity dependence of response of PMGI-encapsulated Pt-AlGaIn/GaN diodes for hydrogen sensing," *IEEE Sensors J.*, vol. 17, no. 18, pp. 5817–5822, Sep. 2017.
- [21] T.-Y. Chen *et al.*, "On an ammonia gas sensor based on a Pt/AlGaIn heterostructure field-effect transistor," *IEEE Electron Device Lett.*, vol. 33, no. 4, pp. 612–614, Apr. 2012.
- [22] S. C. Hung, C. W. Chen, C. Y. Shieh, G. C. Chi, R. Fan, and S. J. Pearton, "High sensitivity carbon monoxide sensors made by zinc oxide modified gated GaN/AlGaIn high electron mobility transistors under room temperature," *Appl. Phys. Lett.*, vol. 98, no. 22, May 2011, Art. no. 223504.
- [23] C. Y. Chang *et al.*, "CO₂ detection using polyethylenimine/starch functionalized AlGaIn/GaN high electron mobility transistors," *Appl. Phys. Lett.*, vol. 92, no. 23, Jun. 2008, Art. no. 232102.
- [24] R. Sokolovskij *et al.*, "Hydrogen sulfide detection properties of p-gated AlGaIn/GaN HEMT-sensor," *Sens. Actuators B, Chem.*, vol. 274, pp. 636–644, Nov. 2018.
- [25] W. Saito, Y. Takada, M. Kuraguchi, K. Tsuda, and I. Omura, "Recessed-gate structure approach toward normally off high-voltage AlGaIn/GaN HEMT for power electronics applications," *IEEE Trans. Electron Devices*, vol. 53, no. 2, pp. 356–362, Feb. 2006.
- [26] J. Zhang *et al.*, "Mechanism of Ti/Al/Ti/W au-free ohmic contacts to AlGaIn/GaN heterostructures via pre-ohmic recess etching and low temperature annealing," *Appl. Phys. Lett.*, vol. 107, no. 26, Dec. 2015, Art. no. 262109.
- [27] R. Vitushinsky, M. Crego-Calama, S. H. Brongersma, and P. Offermans, "Enhanced detection of NO₂ with recessed AlGaIn/GaN open gate structures," *Appl. Phys. Lett.*, vol. 102, no. 17, Apr. 2013, Art. no. 172101.
- [28] C.-T. Lee and Y.-S. Chiu, "Photoelectrochemical passivated ZnO-based nanorod structured glucose biosensors using gate-recessed AlGaIn/GaN ion-sensitive field-effect-transistors," *Sens. Actuators B, Chem.*, vol. 210, pp. 756–761, Apr. 2015.
- [29] S. Huang *et al.*, "High-temperature low-damage gate recess technique and ozone-assisted ALD-grown Al₂O₃ gate dielectric for high-performance normally-off GaN MIS-HEMTs," in *IEDM Tech. Dig.*, Dec. 2014, p. 17.
- [30] S. D. Burnham *et al.*, "Gate-recessed normally-off GaN-on-Si HEMT using a new O₂-BCl₃ digital etching technique," *Phys. Status Solidi*, vol. 7, nos. 7–8, pp. 2010–2012, 2010.
- [31] Y.-L. Chiou, L.-H. Huang, and C.-T. Lee, "Photoelectrochemical function in gate-recessed AlGaIn/GaN metal oxide semiconductor high-electron-mobility transistors," *IEEE Electron Device Lett.*, vol. 31, no. 3, pp. 183–185, Mar. 2010.
- [32] Z. Xu *et al.*, "Fabrication of normally off AlGaIn/GaN MOSFET using a self-terminating gate recess etching technique," *IEEE Electron Device Lett.*, vol. 34, no. 7, pp. 855–857, Jul. 2013.
- [33] R. Sokolovskij *et al.*, "Recessed gate Pt-AlGaIn/GaN HEMT H₂ sensor," in *Proc. IEEE Sensors Conf.*, Montreal, QC, Canada, Oct. 2019, pp. 1–4.
- [34] R. Sokolovskij *et al.*, "Precision recess of AlGaIn/GaN with controllable etching rate using ICP-RIE oxidation and wet etching," *Procedia Eng.*, vol. 168, pp. 1094–1097, 2016.
- [35] T. Hashizume and H. Hasegawa, "Effects of nitrogen deficiency on electronic properties of AlGaIn surfaces subjected to thermal and plasma processes," *Appl. Surf. Sci.*, vol. 234, nos. 1–4, pp. 387–394, Jul. 2004.
- [36] O. Weidemann *et al.*, "Influence of surface oxides on hydrogen-sensitive Pd:GaIn Schottky diodes," *Appl. Phys. Lett.*, vol. 83, no. 4, pp. 773–775, Jul. 2003.
- [37] A. Ortiz-Conde, F. J. García-Sánchez, J. Muci, A. T. Barrios, J. J. Liou, and C.-S. Ho, "Revisiting MOSFET threshold voltage extraction methods," *Microelectron. Rel.*, vol. 53, no. 1, pp. 90–104, Jan. 2013.
- [38] J. P. Ibbetson, P. T. Fini, K. D. Ness, S. P. DenBaars, J. S. Speck, and U. K. Mishra, "Polarization effects, surface states, and the source of electrons in AlGaIn/GaN heterostructure field effect transistors," *Appl. Phys. Lett.*, vol. 77, no. 2, pp. 250–252, 2000.
- [39] H. Seo, T. Endoh, H. Fukuda, and S. Nomura, "Highly sensitive MOSFET gas sensors with porous platinum gate electrode," *Electron. Lett.*, vol. 33, no. 6, p. 535, 1997.



Robert Sokolovskij received the B.S. degree in electronics engineering from Vilnius University, Vilnius, Lithuania, in 2010, and the M.S. degree in electrical engineering from the Delft University of Technology, Delft, The Netherlands, in 2013, where he is currently pursuing the Ph.D. degree. From 2014 to 2018, he was with the State Key Laboratory of Solid-State Lighting, Changzhou, China. Since 2018, he has been a part-time Research Assistant with the Southern University of Science and Technology, Shenzhen, China.

His current research interests include design, fabrication and characterization of wide bandgap gallium nitride (GaN)-based power electronic devices, and chemical sensors.



Jian Zhang received the B.S. degree from Fudan University, Shanghai, China, in 2015, where he is currently pursuing the Ph.D. degree. He is currently visiting Electrical Engineering Department, Katholieke Universiteit Leuven, Leuven, Belgium, and Imec, Leuven. His current research interest includes the electrical properties of metal/semiconductor interfaces for GaN high-electron mobility transistors.



Hongyu Yu (Senior Member, IEEE) received the B.S. degree from Tsinghua University, Beijing, China, the M.Sc. degree from the University of Toronto, Toronto, ON, Canada, and the Ph.D. degree from the National University of Singapore, Singapore. He is currently the Deputy Chair with the Department of Electrical and Electronic Engineering, Southern University of Science and Technology, Shenzhen, China. His current research interests include wide energy gap devices and multilayer chip ceramic capacitors.



Hongze Zheng received the B.S. degree from the South University of Science and Technology, Shenzhen, China, in July, 2019. He is currently working as a Research Assistant with SUSTech. His current research is mainly focused on wide energy gap devices gas sensors.



Pasqualina M. Sarro (Fellow, IEEE) received the Laurea (*cum laude*) degree in solid-states physics from the University of Naples, Italy, in 1980, and the Ph.D. degree in electrical engineering from the Delft University of Technology, The Netherlands, in 1987. From 1981 to 1983, she was a Postdoctoral Fellow with the Division of Engineering, Photovoltaic Research Group, Brown University, Providence, RI, USA. Since then, she has been with the Delft Institute of Microsystems and Nanoelectronics, Delft University of Technology, where she has been responsible for research on integrated silicon sensors and MEMS technology. In 2001, she became an A. van Leeuwenhoek Professor. Since 2004, she has been the Head of the Electronic Components, Materials, and Technology Laboratory. Since 2009, she has been the Chair of the Microelectronics Department, Delft University. She has authored or coauthored over 400 journals and conference papers. In 2006, she became a member of the Royal Netherlands Academy of Arts and Sciences. She is a member of the Technical Program Committee and the International Steering Committee for several international conferences, including the IEEE MEMS, the IEEE SENSORS, Eurosensors, and Transducers. In 2006, she was elected as an IEEE Fellow for her contribution to micromachined sensors, actuators, and microsystems. In 2004, she was a recipient of the EUROSENSORS Fellow Award for her contribution to the field of sensor technology. She is also the Technical Program Co-Chair of the First IEEE Sensors 2002 Conference and the Technical Program Chair of the Second and the Third IEEE Sensors Conference in 2003 and 2004 and the General Co-Chair of the IEEE MEMS 2009. She will act as the General Co-Chair for the IEEE Sensors 2014 and the European TPC Chair for Transducers 2015.



Wenmao Li received the B.E. degree from the Southern University of Science and Technology, Shenzhen, China, in July, 2018, where he is currently pursuing the Ph.D. degree in electronics. His current research interest includes wide energy gap devices and sensors.



Yang Jiang received the B.S. degree from the Southern University of Science and Technology, Shenzhen, China, in 2019. He is currently a Research Assistant with the Southern University of Science and Technology. His research interest includes GaN-based semiconductor materials and devices.



Guoqi Zhang (Fellow, IEEE) received the Ph.D. degree in aerospace engineering from the Delft University of Technology, Delft, The Netherlands, in 1993. He was with Philips, The Netherlands, where he was a Principal Scientist from 1994 to 1996, a Technology Domain Manager from 1996 to 2005, the Senior Director of Technology Strategy from 2005 to 2009, and a Philips Fellow from 2009 to 2013. From 2002 to 2005, he was a Professor with the Technical University of Eindhoven, Eindhoven, The Netherlands. From 2005 to 2013, he was a Chair Professor with the Delft University of Technology. Since 2013, he has been a Chair Professor with the Department of Microelectronics, Delft University of Technology. He has authored over 400 articles including more than 150 journal articles, three books, 17 book chapters, and over 100 patents. His current research interests include heterogeneous micro/nanoelectronics packaging, system integration, and reliability.



Gaiying Yang received the B.S. degree from Northeastern University, Shenyang, China, and the Ph.D. degree from the University of Pierre and Marie Curie (Paris VI), France. She is currently a Professor with the School of Microelectronics and School of Innovation and Entrepreneurship, Southern University of Science and Technology, China. Her current research interests include materials performance and related reliability studies in variety of advanced micro-electronic devices.

Prof. Zhang received the Outstanding Contributions to Reliability Research Award from the European Center for Micro/Nanoreliability, in 2007, the Excellent Leadership Award at EuroSimE, the Special Achievement Award at ICEPT, and the IEEE Components, Packaging, and Manufacturing Technology Society Outstanding Sustained Technical Contribution Award in 2015. He is one of the pioneers in developing the More than Moore (MtM) strategy when he served as the Chair of the MtM Technology team of European's Nanoelectronics Platform in 2005.